Research Article

Ting Su*, Bozhou Xianyu, Wenwen Gao, Yanli Gao, Pingqiang Gao, and Cuiying Lu*

High removal efficiency of volatile phenol from coking wastewater using coal gasification slag via optimized adsorption and multi-grade batch process

https://doi.org/10.1515/gps-2022-8130
received October 21, 2022; accepted December 13, 2022

Abstract: Powder adsorbent made by coal gasification slag (CGS) was used to adsorb pollutants from coking wastewater (CW). This study initially focused on the removal efficiency of volatile phenol, NH_3–N, and chemical oxygen demand (COD) from CW. The removal rate of volatile phenol increased from 48.90% to 70.50% after acid precipitation of CW by 4.0 mL reagent of sulfuric acid (3.0 M) and optimization of adsorption process by central composite design-response surface methodology with optimized conditions. Volume ratio of liquid and solid adsorbent ($V_{L/S}$) and pH were the significant factors in the adsorption process. Batch experiment improved the volatile phenol, NH_3–N, and COD removal rate to 85.1%, 41.6%, and 77.3%, respectively. Multi-grade batch process in grade 3 made a further promotion of pollutants removal rate as 98.5%, 73.6%, and 80.5%, respectively. Scanning electron microscope-energy dispersive spectrum and Fourier-transform infrared spectrometer were used to confirm the adsorption effect. CGS-based adsorbent for CW treatment has potential advantages due to the features of good adsorption performance and low cost.

Keywords: removal rate, coal gasification slag, coking wastewater, response surface method, multi-grade batch process

Abbreviations

A-CGS	CGS pretreated by alkali solution
Ac-CGS1	CGS pretreated by nitric acid
Ac-CGS2	CGS pretreated by hydrochloric acid
ApCW	CW after acid precipitation treatment
CGS	coal gasification slag
CGS-F	fine coal gasification slag
CGS-R	rough coal gasification slag
COD	chemical oxygen demand
CW	coking wastewater
DCW	raw wastewater diluted 50 times
NHCs	N-heterocyclic carbenes
PAHs	polycyclic aromatic hydrocarbons
PCBs	polychlorinated biphenyls
$V_{L/S}$	volume ratio of liquid and solid adsorbent
A	pH
B	$V_{L/S}$
C	processing time
D	particle size of adsorbent

1 Introduction

Coal chemical industry plays a very important role in the economic construction and social development in China. By the end of June 2022, the growth rate of raw coal output was up to 15.3% as shown in Figure 1a [1]. Coal gasification and coking industry consume large amount of coal [2–4], leading to production of coal gasification slag (CGS) and coking wastewater (CW) in abundance. Numerous pollutants including ammonia, cyanide,

* **Corresponding author: Ting Su,** School of Chemistry and Chemical Engineering, YuLin University, Shaanxi Key Laboratory of Low Metamorphic Coal Clean Utilization, Yulin 719000, China, e-mail: st1010ivy@126.com
* **Corresponding author: Cuiying Lu,** School of Chemistry and Chemical Engineering, YuLin University, Shaanxi Key Laboratory of Low Metamorphic Coal Clean Utilization, Yulin 719000, China, e-mail: 345524852@qq.com
Bozhou Xianyu, Wenwen Gao, Yanli Gao, Pingqiang Gao: School of Chemistry and Chemical Engineering, YuLin University, Yulin 719000, China

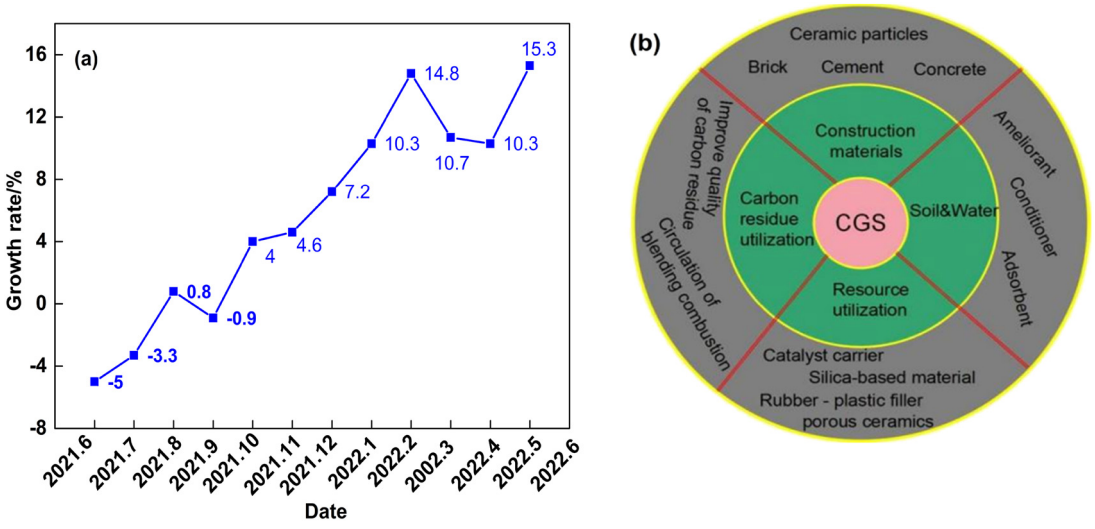

Figure 1: Resource situation: (a) growth rate of raw coal output and (b) comprehensive utilization of CGS.

phenols, other organic compounds, and toxic components are present in CW [5–7]. High organic pollutant load, strong bio-inhibitive, carcinogenic properties, and complex composition of the CW make it refractory for conventional biological treatment [8]. The organic pollutants typically include benzene derivatives, phenolic compounds, amines, polycyclic aromatic hydrocarbons (PAHs), N-heterocyclic carbenes (NHCs), organic nitriles, and polychlorinated biphenyls (PCBs). Among these, refractory organics of NHCs, PAHs, and PCBs account for a considerable part of chemical oxygen demand (COD) in CW [9]. It is a threat to ecological environment and human health because of high toxicity and difficulty to degrade. Traditional methods for CW treatments include biological treatment [10], advanced oxidation [11], and membrane separation [12]. By contrast, biological treatment is an economical secondary wastewater treatment. Whereas, several pollutants remaining in the process including PAHs, halogenated organics, and long-chain hydrocarbons, the high value of B/C as well as the low processing efficiency [13–17], make it necessary for the additional advanced treatment because of the inappropriate discharge of the treated CW [18]. Meanwhile, the low removal rate of pollutants, secondary pollution, high energy consumption, and high cost makes it difficult to remove the impurities with stable molecular structure via the traditional methods. Thus, the disadvantages of current technology can be summarized in two aspects: (i) the content of volatile phenol and other pollutants like NH_3–N, COD, and phenolic compounds in the CW are still high after treatment and with high biological toxicity [19–24]; (ii) large scale promotion of current technology are seriously restricted by the high investment costs, high operating costs, harsh reaction conditions, and unstable operation. Additionally, adsorption is an effective physico-chemical method extensively concerned by researchers and many studies have been done on wastewater adsorption [25–30].

Commercial activated carbon as a common adsorbent is usually applied in the treatment of wastewater, while high adsorption capacity is coupled with high costs [31]. Even though variable activated carbon materials are available, the molecular size and the functional groups of pollutants in CW limit the adsorption performance. Therefore, lower energy consumption and higher adsorption efficiency of the activated carbon was developed such as activated coke [32], lignite activated coke [33], and coal-based adsorbents [34]. The COD removal rate of these adsorbents were optimistic with 74.0–85.9%, but some of the operations are little more complicated. Therefore, the adsorbent selective decision was made taking into account the cost, safety, accessibility, and reuse in addition to the adsorption capacity [35]. CGS is a kind of solid waste with pore structures which was generated from the gasification process [36]. The comprehensive utilization of CGS was shown in Figure 1b. The CGS, including the rough slag (CGS-R) and fine slag (CGS-F), can be explored as the adsorbent for CW, which was inspiring from another solid waste utilization of coal fly ash (CFA). CFA is a valuable industrial solid waste, but conventional methods used for its disposal can lead to serious and long-lasting environmental issues [37]. There is a simple utilization method of CFA, which enables direct use of CFA as adsorbent to treat CW. When the dosage was 40.0 $g \cdot L^{-1}$, processing time was 240 min, pH was 7, and temperature was 293 K,

the COD removal rate was 89.9%. In view of the good adsorption performance of CFA [38], CGS has been employed as adsorbent of CW in this work after chemical pretreatment.

Then, the adsorption process was carried out in batch systems with consideration to the number of required factors to save time and decrease the consumption of reagents and material, optimizing the process in order to achieve the best probable response, so the optimization process is the key solution. Central composite design (CCD) is established as the most extensively used optimization method for the adsorption process because of the benefits of optimizing several factor problems with the best number of test runs according to the design of experiment [39]. The existing research on the adsorption process optimization has been mostly focusing on CCD, although the number of experiments may be large, and adsorption process was designed according to the response surface methodology (RSM) using CCD [40].

The objectives of this work are: (i) to select the potential adsorbent by chemical treatment of CGS and to determine the acid precipitation conditions of CW; (ii) to investigate the effect of pH, volume ratio of liquid and solid ($V_{L/S}$), processing time, and particle size of the adsorbent and to optimize the adsorption process by CCD-RSM; (iii) to conduct batch experiment and multigrade process to improve the pollutants removal rate.

2 Materials and methods

In this study, three experiment units were conducted based on volatile phenol removal efficiency from CW such as pretreatment of CGS, acid precipitation of CW, and adsorption process of CW. The details of the units are provided in the following sections.

2.1 Raw materials

The CW used in the experiments was obtained from a coke plant in Shaanxi province (China). The quality parameters of CW are shown in Table 1.

Table 1: Quality parameters of CW

Parameter	COD_{Gr} ($mg \cdot L^{-1}$)	COD ($mg \cdot L^{-1}$)	NH_3–N ($mg \cdot L^{-1}$)	Volatile phenol ($mg \cdot L^{-1}$)	pH	BOD_5 ($mg \cdot L^{-1}$)	Color/times
Average value	50,000.0	50,065.2	4,500.2	6,000.3	7.8	6,200.5	700.0

COD_{Gr}: determination of the COD by dichromate process method; COD: determination of the COD by rapid digestion spectrophotometric method; BOD_5: biochemical oxygen demands within 5 days.

Table 2: Proximate analysis and ash composition of samples

	Raw coal	CGS-F	CGS-R
Proximate analysis (% p/p)[a]			
Moisture	1.41	9.38	5.58
Volatile matter	35.93	14.61	21.51
Fixed carbon	56.67	27.36	19.10
Ash	5.99	48.65	53.81
Composition of ash (% p/p)			
Al_2O_3	19.30	16.10	9.95
SiO_2	44.80	29.14	28.84
CaO	16.72	20.02	28.37
Fe_2O_3	8.09	17.98	20.31
Na_2O	0.16	1.27	1.53
MgO	1.46	4.30	2.91
CuO	0.84	0.03	0.03
others	8.63	11.16	8.06

[a]Dry and ash free basis.

For the purpose of comparison, CGS-F and CGS-R were both involved in this study. Prior to their initial use, all the samples were rinsed with water to remove the possible impurities inside, and vacuum desiccated at 363 K to achieve a constant weight. The proximate analysis and ash composition of the samples are summarized in Table 2, and the morphology characteristics are shown in Figure 2.

2.2 Pretreatment method

The CW was pretreated by two methods. One is only filtration to remove solid impurities and diluted 50 times for usage, which was labeled as DCW. The other method is acid precipitation. CW was first aerated by oxygen pump for 3 h, then transferred to a flask into which sulfuric acid and water were added and kept for 12 h. Here a series concentration of sulfuric acid of 1.0, 1.5, 2.0, 2.5, and 3.0 M was used, and the volume set was 1.0, 2.0, 3.0, 4.0, and 5.0 mL. Selective results will be discussed later in detail. Finally, the water was filtered and labeled as acid precipitated coking wastewater (ApCW).

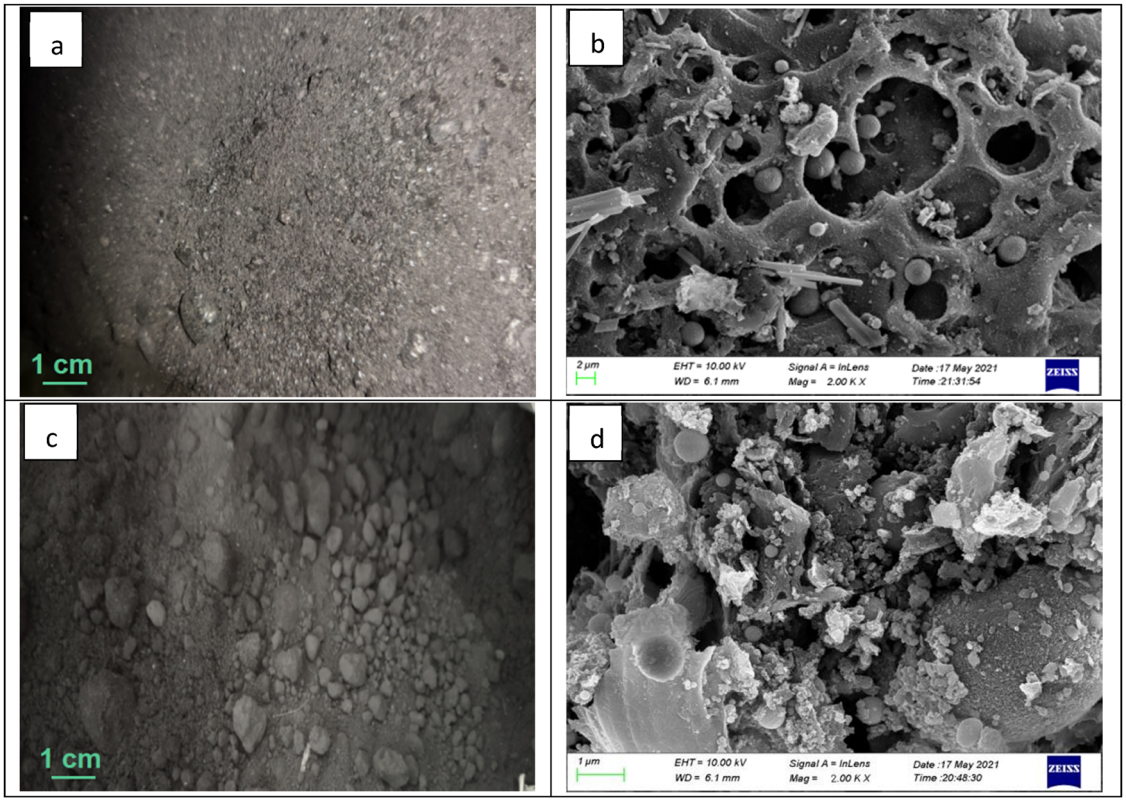

Figure 2: (a) Photo of CGS-F, (b) SEM image of CGS-F, (c) photo of CGS-R, (d) SEM image of CGS-R.

The CGS-F and CGS-R were both crushed and screened to homogeneous powder with three particle sizes of 180, 150, and 125 µm, which were signed as F180, F150, F125, R180, R150, and R125, respectively. The selected 6 samples were severally soak in 2 wt% sodium hydroxide (NaOH), nitric acid (HNO_3), and hydrochloric acid (HCl) solution for 3 h, and then rinsed to neutral by distilled water. After drying, they were marked as sample groups of A-CGS, Ac-CGS1, and Ac-CGS2 (HCl), respectively.

2.3 Experimental procedure

The experiments were conducted at a temperature of 293 K controlled by water bath and did not adjust any more in this study. The volume of water sample was 50.0 mL per time in a 250.0 mL flask. The dosage of adsorbent was determined by a certain experimental condition ($V_{L/S}$ = 1, 2, and 3). The solution pH was adjusted using 0.1 mol·L^{-1} NaOH or HCl. Stirring speed was 500 rpm, the adsorption time was 3–7 h. The schematic of the investigated process is shown in Figure 3.

2.4 Apparatus and analysis

The sodium hydroxide (NaOH, 93%), hydrochloric acid (HCl, 35–37%), and nitric acid (HNO_3, 65–68%) were purchased from HongYan reagent company (Tianjin, China). Potassium bromate ($KBrO_3$, >99%), potassium bromide (KBr, >99%), and potassium iodide (KI, >99%) were acquired from Xiya chemical technology Co., Ltd (Shandong, China). Sodium thiosulfate ($Na_2S_2O_3$, >99%), potassium ferricyanide ($K_3[Fe(CN)_6]$, >99%), and 4-aminoantipyrine ($C_{11}H_{13}N_3O$, >99%) were supplied by Xi'an reagent factory (Xi'an, China). The test reagents of NH_3–N (LH-N2N3-100) and COD (LH-D/E-100) were both provided by Lian-Hua Tech Co., Ltd (Beijing, China). All chemicals were of analytical grade and used as received without any further purification. The oxygen pump with max volume of 2.5 L·min^{-1} was bought from Sensen industrial Co., Ltd (HP-100, Zhejiang, China).

The morphology and structure of the adsorbents were characterized by scanning electron microscope (SEM, Carl Zeiss Sigma 300, Germany) and Fourier-transform infrared spectroscopy (FTIR, Shimadzu-8400S spectrometer, Japan). The spectra were recorded from 4,000 to 500 cm^{-1} using a

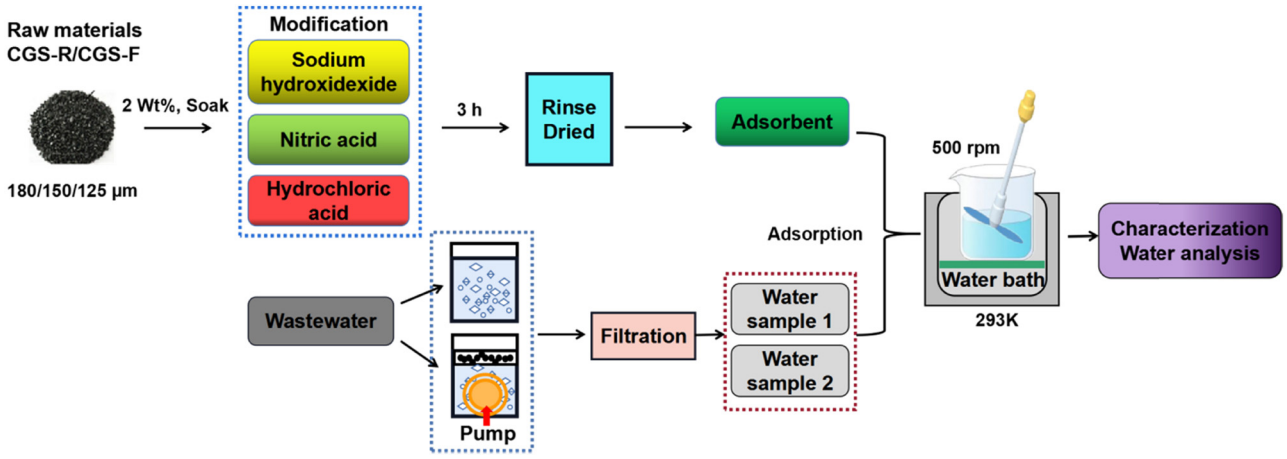

Figure 3: The schematic of the investigated process.

KBr window. 4-aminoantipyrine spectrophotometric method was adopted to determine the volatile phenolic compounds according to the national standard of China HJ503-2009. The limit of detection was 0.01 mg·L^{-1}, limit of quantitation was 0.04 mg·L^{-1}, which were calculated by the standard deviation of the response and the slope of calibration curves according to the literature [41–43]. The COD and NH_3–N were tested by water quality analyzer (5B-3B-V11) from LianHua science and technology Ltd (Beijing, China). Values of COD were determined by rapid digestion spectrophotometric method referred to national standard of HJ T399–2007, and the test method of NH_3. Moreover, the removal rate of pollutants were calculated from Eq. 1 as follows:

$$R = \frac{C_0 - C_1}{C_0} \times 100\% \quad (1)$$

where C_0 is the initial concentration of the pollutants (mg·L^{-1}) and C_1 is the concentration of the pollutants after treatment (mg·L^{-1}).

2.5 Response surface experiments design

An experimental design for the adsorption process was required to obtain optimized operation parameters as well as reduce the experimental cost. Factors adopted here were pH (A), $V_{L/S}$ (B), processing time (C), and particle size of the adsorbent (D). There are three levels for each factor as shown in Table A1 (in Appendix). The orthogonal array designed by JMP software is listed in Table A2, this method reduced the experimental number from $3^4 = 81$ to L_{15} (3^4) = 15.

3 Results and discussion

3.1 Selective experiment

Pollutants removal efficiency was evaluated by the removal rate of volatile phenol, COD, and NH_3–N using four group adsorbents (CGS, A-CGS, Ac-CGS1, and Ac-CGS2). The operation temperature was 293 K, the DCW volume was 50.0 mL, the pH was 7.0, the processing time was 3 h, and the $V_{L/S}$ was 3. The operation conditions as well as the removal results are shown in Figure 4.

It is clear that Ac-CGS2 group exhibited the best pollutant removal performance for each species than the other adsorbents, and the CGS-F was better than CGS-R. The particle size has an effect on adsorption, for F group samples, the smaller particle size shows better pollutants adsorption effect. Sample F125 of Ac-CGS2 group (labeled as Ac-CGS2-F125) got the maximum removal rate of COD, NH_3–N, and volatile phenol as 30.29%, 30.66%, and 48.90%, respectively. The original pore structures of CGS ensured certain adsorption capacity of pollutant, so the highest removal rate of volatile phenol could be achieved at 42.50% by sample F125 in the group of CGS. Theoretically, acid soak process increased the acidic functional groups which is beneficial to pollutant adsorption, hence the Ac-CGS2 group emerged as a large advantage in pollutant adsorption process. Therefore, the F series samples in Ac-CGS2 group (labeled as Ac-CGS2-F) will be selected for optimization in the subsequent experiments.

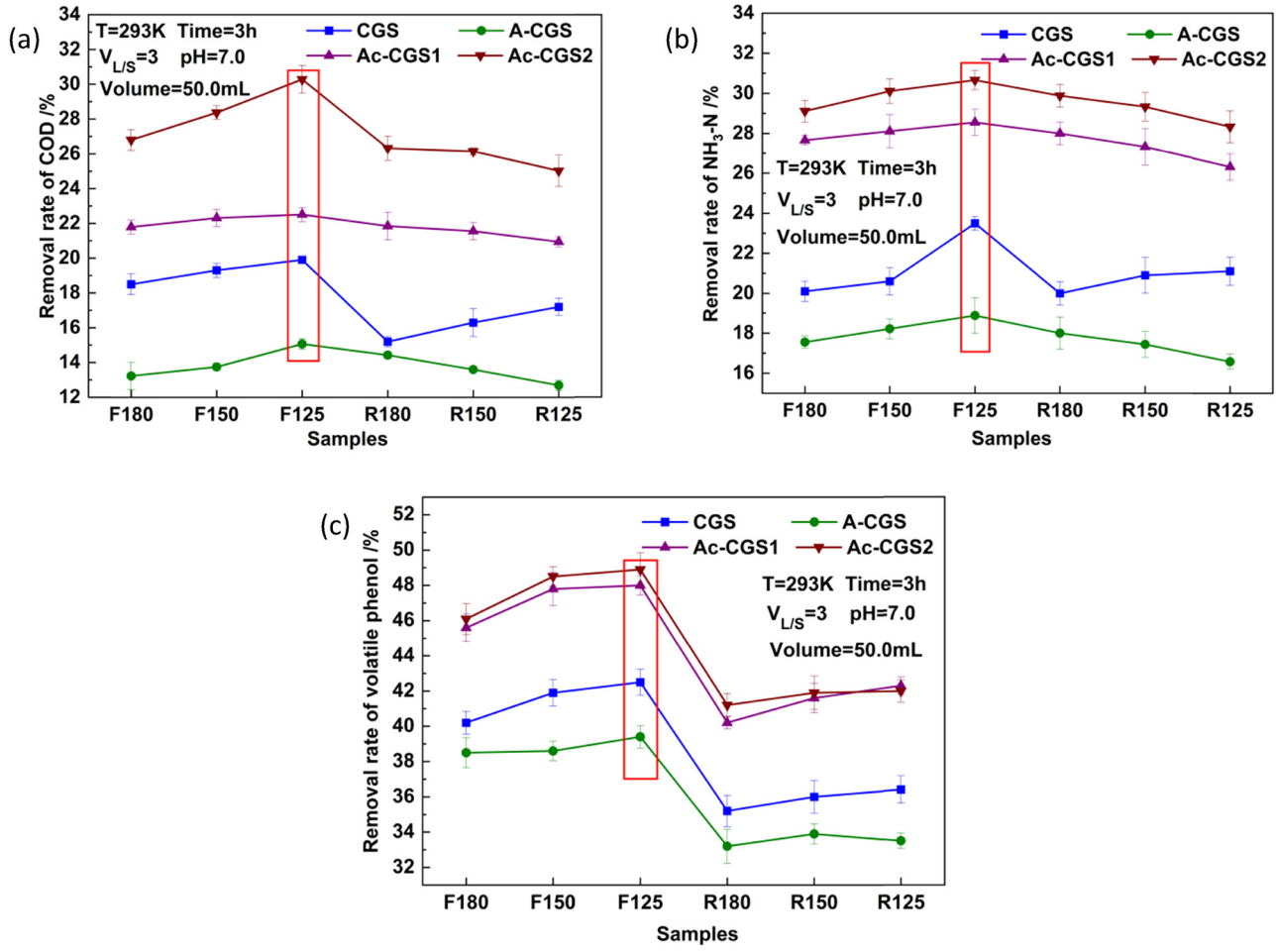

Figure 4: The pollutants removal rate of different adsorbents: (a) the removal rate of COD, (b) the removal rate of NH_3–N, and (c) the removal rate of volatile phenol.

3.2 Acid precipitation experiment

Acid precipitation experiment was conducted at room temperature as introduced in Section 2.2, 5 set experiments with different sulfuric acid volume (in order of 1.0–5.0 mL) were performed for each concentration. The amount of water sample taken was 50.0 mL in each set. The phenomena of experimental process are shown in Figure 5, and the experiment results are displayed in Figure 6.

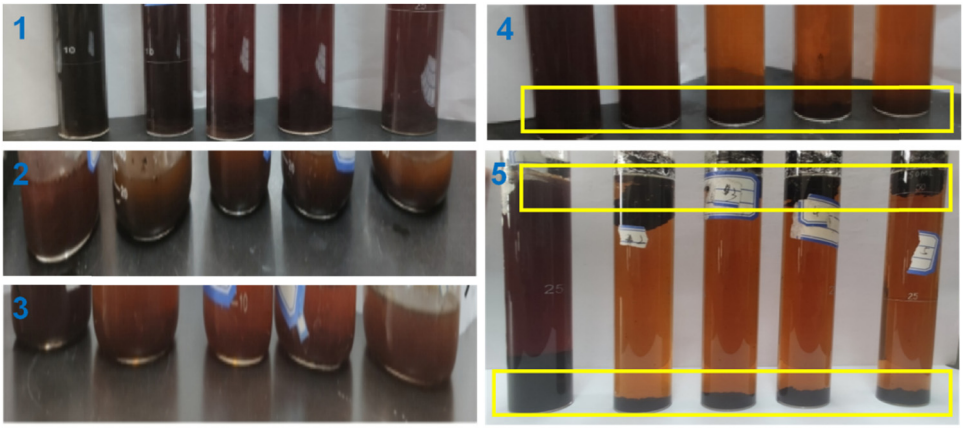

Figure 5: The experimental phenomena at different conditions. The concentration of sulfuric acid in photo 1, 2, 3, 4 and 5 was 1.0 M, 1.5 M, 2.0 M, 2.5 M and 3.0 M, respectively. The volume of sulfuric acid in each photo from left to right in turn as 1.0, 2.0, 3.0, 4.0, 5.0 mL.

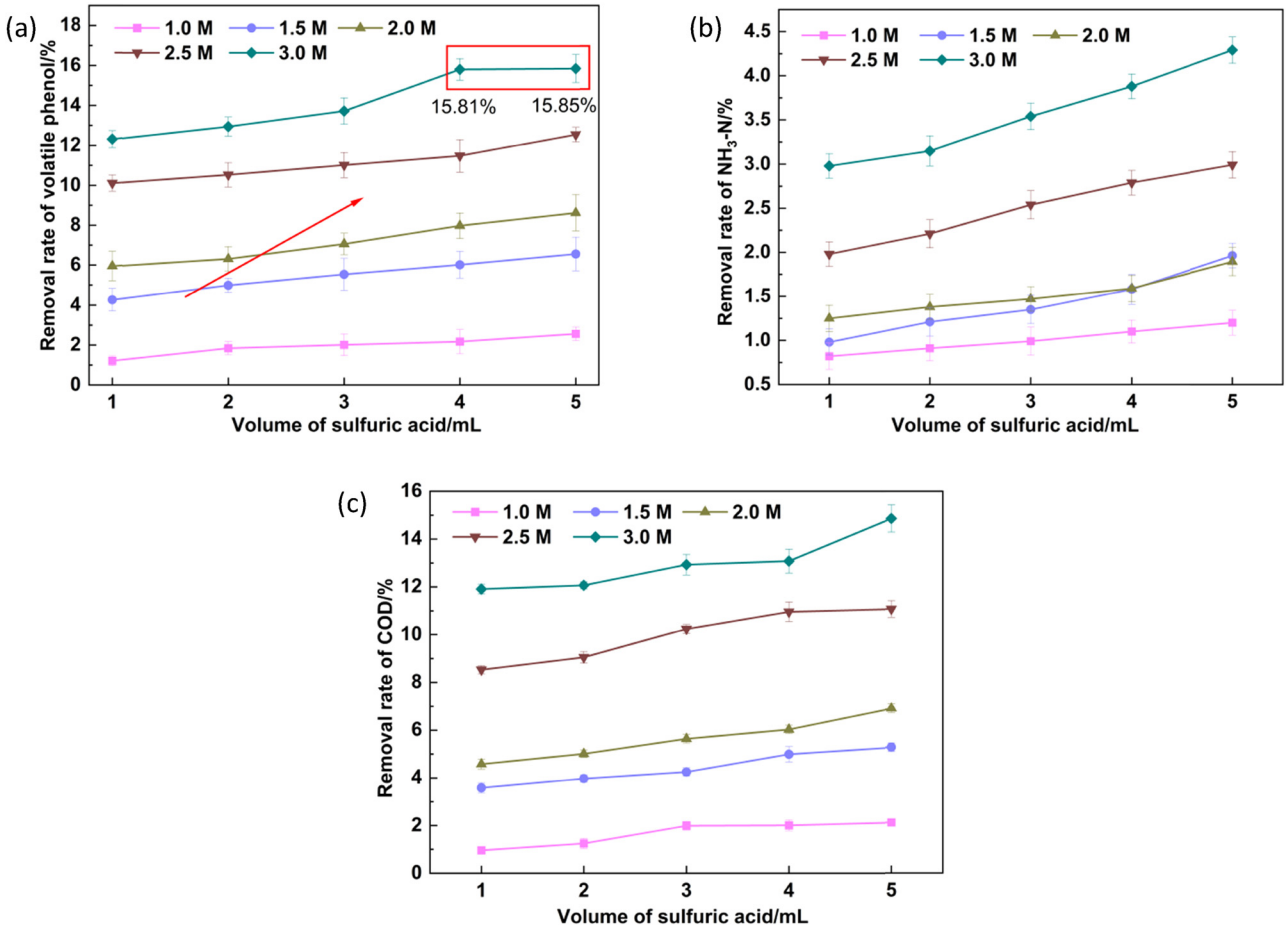

Figure 6: The removal rate of pollutants at different concentrations of sulfuric acid: (a) the removal rate of volatile phenol, (b) the removal rate of NH_3–N, and (c) the removal rate of COD.

Table 3: Volatile phenol removal rate of samples at different conditions

No.	Condition	Removal rate of volatile phenol (%)
1	A1B1C1D3	62.1
2	A3B1C1D3	59.1
3	A3B3C2D1	60.3
4	A2B2C3D3	61.4
5	A1B3C1D1	68.5
6	A3B3C2D1	63.2
7	A1B1C2D1	63.4
8	A1B3C2D2	69.7
9	A3B3C2D2	62.5
10	A2B1C1D1	60.0
11	A1B2C2D1	63.8
12	A2B1C2D2	61.8
13	A2B3C2D3	63.4
14	A2B2C1D2	62.1
15	A3B1C2D1	59.3

As is evident from Figure 5, more precipitations appeared in photos 4 and 5, which have higher concentration and larger volume of sulfuric acid. With 2.0–5.0 mL addition of 3.0 M sulfuric acid, there were brown substances aggregated at the bottom and top of the test tube, as well as above the liquid level, indicating that more volatile phenols were converted. The phenomena was consistent with the results in Figure 6. The removal rate of volatile phenol increased from 1.21% (1.0 mL, 1.0 M, sample marked as Ap11) to 15.81% (4.0 mL, 3.0 M, Ap43) and 15.85% (5.0 mL, 3.0 M, Ap53). Higher volatile phenol removal rate was obtained by Ap43 and Ap53. The aim of acid precipitation process is to convert the volatile phenolic compounds to phenol quinone compounds, the removal rate of Ap43 was close to Ap53, therefore the volume of 3.0 M sulfuric acid was determined as 4.0 mL to save the reagent. Meanwhile, the removal rate of NH_3–N and COD were 3.88% and 13.08%, respectively.

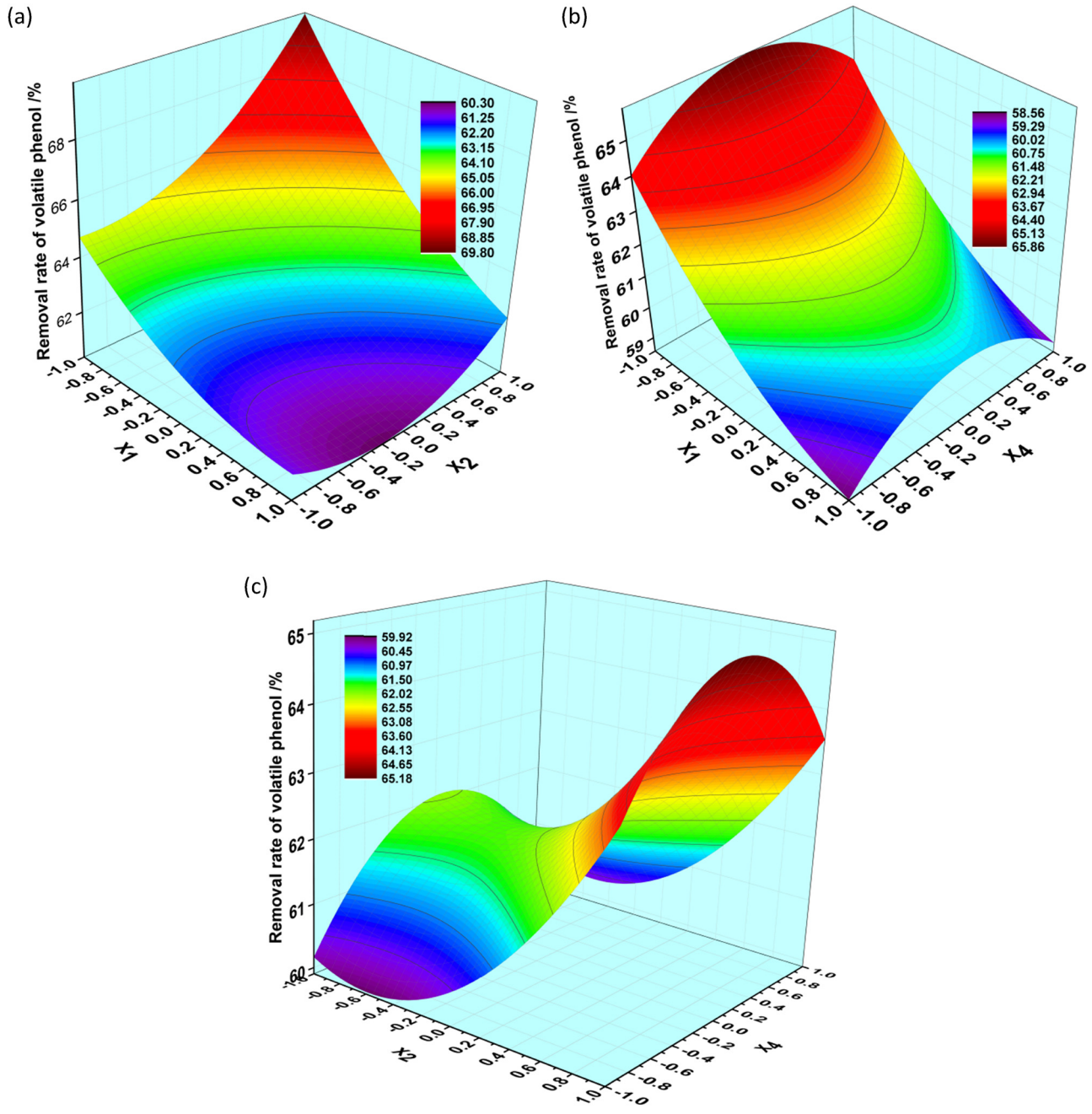

Figure 7: 3-D plot showing the effect of X_1, X_2, and X_4 on the removal rate of volatile phenol: (a) the effect of X_1 and X_2, (b) the effect of X_1 and X_4, and (c) the effect of X_2 and X_4.

3.3 Result of design

The adsorbents were selected as Ac-CGS2-F, particle size of the adsorbents remained a concerned factor in the optimization experiment. The results for 15 runs are shown in Table 3. On comparison, the sample of No. 8 achieved the maximum removal rate (69.7%) of volatile phenol. At the same time, the optimum conditions were also revealed. The serials of A1B3C2D2 means the pH and $V_{L/S}$ values were 3, the processing time was 5 h and the particle size was 150 μm. And the sample was labeled as Ac-CGS2-F150 for later use.

3.3.1 Analysis of model

The stepwise regression method was adopted to analyze the experimental data in Table 3. Analysis of variance

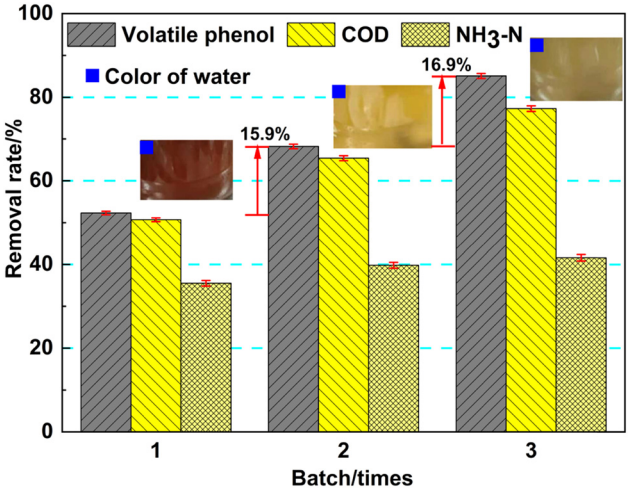

Figure 8: Removal rate of pollutants and color of water in batch experiment.

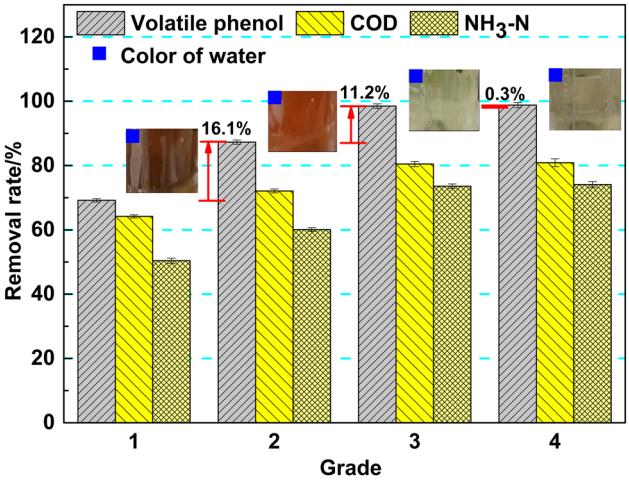

Figure 9: Removal rate of pollutants and the color of water in multi-grade batch process.

and significance test for the regression model are listed in Tables A3 and A4, respectively. The R^2 is 0.9955, F-value is 37.0758, and the P-value is 0.0266 in Table A3, which indicated that the stepwise regression model was suitable for analysis of the experimental data. Hence, the selected model was applicable for analyzing and optimizing the adsorption process. There are four significant factors marked as "*" in Table A4, the most significant of these factors are the pH and $V_{L/S}$ in the adsorption process, and the sequence for these factors was A > B > D^2 > A × B > C > D. Quadratic terms stated that the interaction of these factors are not merely a simple linear correlation.

3.3.2 RSM optimization and verification

The RSM method was employed to analyze the experimental data in Table 3. The quadratic regression surface model was established after eliminating the non-significant items. And the model for removal rate of volatile phenol can be calculated by the obtained quadratic regression equation given by Eq. 2 as follows:

$$R = 62.2317 - 2.724X_1 + 1.549X_2 + 0.281X_3 + 0.136X_4 + 0.885X_1^2 - 0.977X_1X_2 + 1.389X_2^2 - 0.114X_1X_3 - 0.297X_2X_3 - 0.090X_2X_4 + 0.356X_3X_4 - 1.680X_4^2 \quad (2)$$

where X_1, X_2, X_3, and X_4 are equal to (pH-5)/2, $V_{L/S}$-2, (processing time-5)/2, and (particle size-150)/30.

Meanwhile, interaction effect among these three key factors were explored by three-dimensional RSM of the quadratic polynomial regression equation in order to attain the optimization conditions for adsorption. The effect of X_1, X_2, and X_4 on the removal rate of volatile phenol are shown in Figure 7.

The convex surfaces can be clearly seen on the response surface in Figure 7, which means that the model has a stable maximum point in the test range. The removal rate of volatile phenol fluctuated within 58.56–69.80%, each removal rate has the corresponding conditions and can be verified according to this process condition. Three parallel experiments of certification were carried out according to the optimal process conditions, and the volatile phenol removal rate of 69.9%, 70.2%, and 71.4% were obtained. The average removal rate was 70.50%, which is consistent with the predicted value. Therefore, the optimal condition from the RSM method is believable.

3.4 Batch experiment

The removal rate of volatile phenol needs to be improved persistently, hence the bath experiment was carried out to make efforts for this purpose. All the experimental operations were performed according to the optimal conditions, but divided the adsorbent into three equal parts and added in three batches. The experimental results are shown in Figure 8.

A gradual increasing tendency of pollutants removal rate was observed as the batches increased in Figure 8. With the one third of adsorbent at the first batch, the removal rate of volatile phenol, NH_3–N, and COD was 52.3%, 50.7%, and 35.5%, respectively. The removal rate of volatile phenol was lower than the average value of 70.50% obtained in Section 3.3.2 because of the limitation of adsorption capacity. The removal rate of volatile phenol increment was 15.9% in the second batch, the removal rate of 68.2% was almost as high as the optimal value only by

two thirds of the adsorbent. Meanwhile, removal rate of NH_3–N and COD also increased to 39.8% and 65.4%. In the third batch, removal rate of volatile phenol was 85.1% with the increment of 16.9% compared to the second batch. At the same time, removal rate of NH_3–N and COD were 41.6% and 77.3%. The color of water was getting more and more clear and transparent reflecting the improvement of adsorption performance. Batch experiment can greatly improve the removal rate of pollutants due to the adsorption capacity and release of active sites in batches, thereby enhancing the competitive adsorption of pollutants and water.

3.5 Multi-grade batch process

Because of the pollutants removal rate progress achieved in the batch experiment, the multi-grade batch process intended to provide further improvement. The grade of process was set as 4, and the experiment was conducted with the optimal conditions. The experimental results are shown in Figure 9.

The significant improvement in volatile phenol removal rate are displayed in Figure 9. A rapid rise in the volatile phenol removal rate (from 69.2% to 87.3%) was observed at the grade 2 process with increment of 16.1%, as well as the increased removal rate of NH_3–N and COD from 64.2% to 72.1% and 50.4% to 60.1%, respectively. Only smaller increments of 11.2% occurred in grade 3 process, but the volatile phenol removal rate has already reached 98.5%, the color of water was greatly different from the beginning and became clear or transparent at this moment. Meanwhile, the removal rate of NH_3–N and COD were 73.6% and 80.5%. Few increments were acquired after the grade 4 process, therefore, 3 grade of process was determined for sake of adsorption efficiency. The fresh adsorbent at each grade provided more surface area and active sites to increase the pollutants removal rate [44]. The removal effect accumulated by every single grade contributed to the most higher removal rate (more than 98%) of volatile phenol.

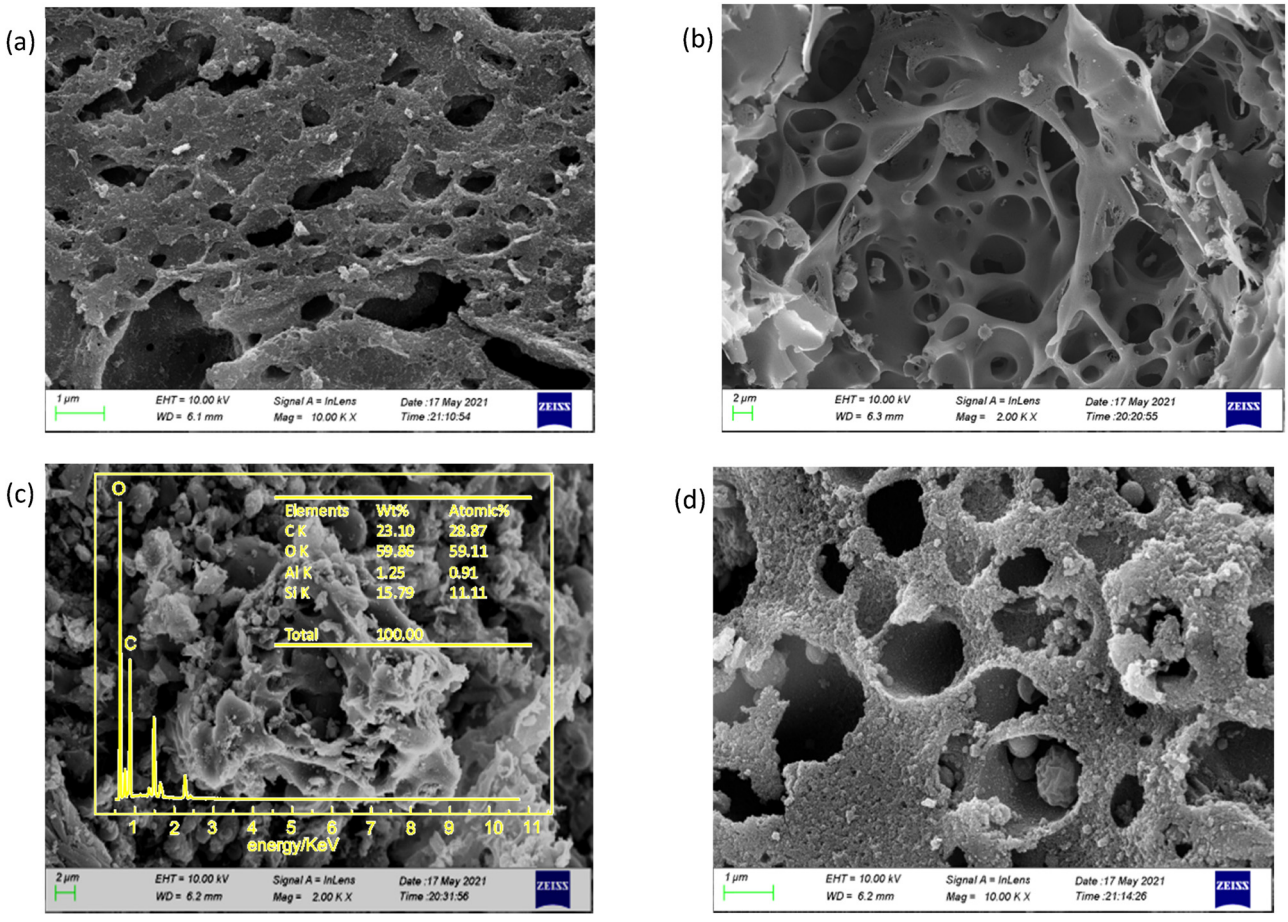

Figure 10: SEM images of Ac-CGS2-F150 before and after adsorption: (a) before, Ac-CGS2-F150 × 10.0 K, (b) before, Ac-CGS2-F150 × 2.0 K, (c) after, Ac-CGS2-F150 × 2.0 K, and (d) after, Ac-CGS2-F150 × 10.0 K.

3.6 SEM-energy dispersive spectrum analysis for adsorbent

SEM images of Ac-CGS2-F150 before and after adsorption process are presented in Figure 10. After soaking in HCl solution, rough morphology of matrix surface are shown in Figure 10a; meanwhile, clean porous structure and open-framework structure (Figure 10b) illustrate that some of the mineral impurities in the pore structure have been cleaned up. After experiencing the adsorption process, some of the pore structures are covered (Figure 10c) and filled (Figure 10d) with attachments. Chemical analysis by EDS (Figure 10c) in the SEM instrument detected C (23.10 wt%) and O (59.86 wt%), which can be attributed to the adsorption pollutants including volatile phenol in the whole process.

3.7 FT-IR analysis

Chemical nature changes in Ac-CGS2-F150 before and after adsorption process are recorded by FT-IR spectra in Figure 11. The bands in the range of 1,300–1,000 cm^{-1} can be assigned to the in-plane bending of the C–H, bands at 1,635 cm^{-1} correspond to C=C stretching bond. The band at 2,000 cm^{-1} is assigned to the C=O stretch bond, and the presence of the OH group is indicated by a broad, weak band at 3,480 cm^{-1}. In Figure 11b, several major peaks in the range 500–2,100 cm^{-1} are seen in the spectrum of samples specifically at around 2,010, 1,630, 1,380, 1,270, 1,100, 875, 670, and 612 cm^{-1} (as indicated in the figure), confirming the response enhancement of characteristic peak by the presence of pollutants functional groups after adsorption process.

3.8 Adsorption performance and mechanism

Removing pollutants from wastewater by adsorbents is a kind of physical adsorption process, CGS possesses the adsorption properties due to its own pore structure. The pretreatment with acid soak was designed to increase the pore structures and enrich the functional groups of adsorbent. Adsorption performance is widely believed to be associated with the functional groups of adsorbent [45]. It is well-known that surface oxygen-containing functional group can form aggregates with pollutant molecules via intermolecular forces and/or chemical reaction, significantly affecting the adsorption of pollutants including phenols [46]. Meanwhile, the acidic environment favored the adsorption of another anionic material [47], and the strong electrostatic interactions between the ionized pollutants species and the positively charged adsorbent surface resulted in the highest volatile phenol removal rate at pH of 3.0. Multi-grade batch process accumulated every single batch adsorption performance, the more the adsorption capacity, the active sites were released in batches by the fresh adsorbent. The volatile phenol removal rate of 98.5% in this work is relatively high compared with other similar studies about adsorption of CW, some of which are listed in Table 4.

The coal-based adsorbents such as magnetic activated carbon (MAC), sludge-derived activated carbon (SAC), commercial activated carbon (CAC), lignite activated carbon (LAC), and coal fly ash (CFA) applied in

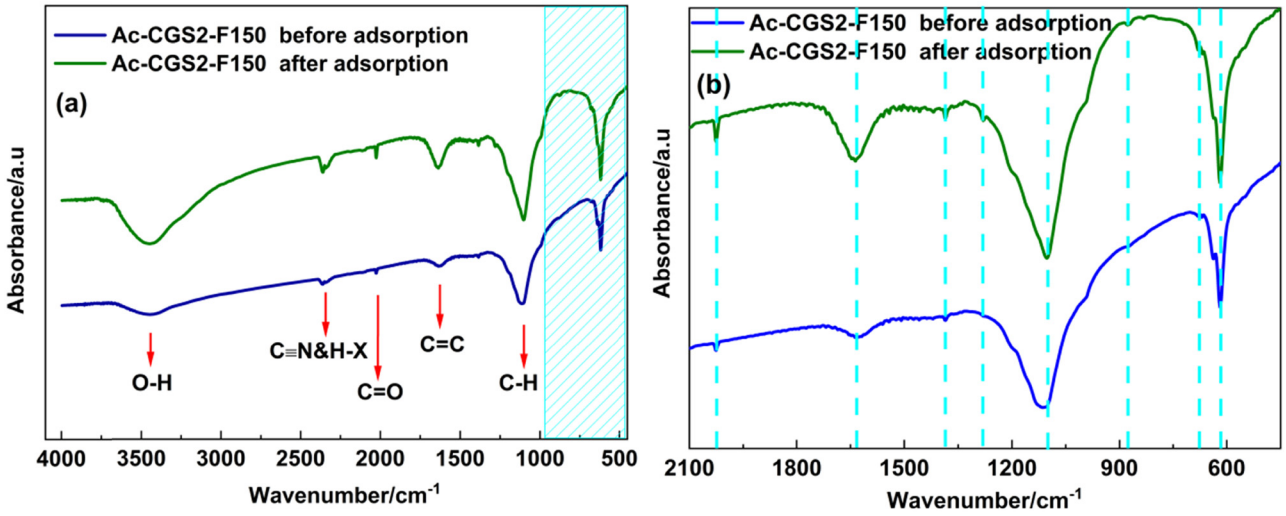

Figure 11: The FT-IR spectra of Ac-CGS2-F150 before and after adsorption: (a) 4,000–500 cm^{-1} and (b) 2,100–500 cm^{-1}.

Table 4: Adsorption performance of phenol or COD from CW presented in published papers

Adsorbent	Conditions	Removal rate	Ref.
Ac-CGS-F150	Volume: 50 mL; pH: 3; processing time: 5 h; particle size: 150 μm; $V_{L/S}$: 3	Phenol: 98.5% COD: 80.5%	This work
Fe-BiOBr/rGA	Processing time: 30–50 min; pH: 5; H_2O_2: 50 μL; dosage: 50 mg; C_{phenol}: 20–50 ppm	Phenol: 99% COD: 48%	[48]
MAC	Dosage: 0.5 g; volume: 100 mL; shaken speed: 200 rpm; temperature: 25°C; processing time: 3 h	COD: 78.57%	[49]
Coal-based adsorbents	Volume: 30 L; agitate speed: 100 rpm; time: 30 min; temperature: 298 K; dosage:140 $g{\cdot}L^{-1}$	COD: 74.0%	[34]
SAC	Dosage: 7.0 $g{\cdot}L^{-1}$; pH: 7.2–7.8; aerobic reaction time: 6 h	COD: 96.0%	[18]
CFA	Dosage: 40.0 $g{\cdot}L^{-1}$; processing time: 240 min; pH: 7; temperature: 293 K	COD: 89.9%	[38]
CAC	Volume: 150 mL; temperature: 25°C; initial pH: 7.0; processing time: 24 h; shaking speed: 200 rpm	COD: 80.0%	[32]
LAC	Dosage: 0.3 g; volume: 100 mL; air-bath shaker speed: 150 rpm; temperature: 293 K; processing time: 48 h; pH: 7.0	Phenol: 85.9%	[33]
AMPS-Am/MIP	Dosage: 20 mg; temperature: 298 K; concentration: 50 $mg{\cdot}L^{-1}$; volume: 40 mL; processing time: 180 min; pH: 8	Phenol: 96.6%	[50]

adsorption of CW were mainly concerned on the removal rate of phenol and COD. Ac-CGS-F150 has great advantages in phenol removal efficiency compared with the adsorbent in list, and little difference in COD removal rate. These adsorbents with the features of effective recovery, good separation performance, better removal efficiency of total phenols content, total organic carbon, total nitrogen, plus toxicity and stable regeneration ability and so on contributed to the development of CW treatment. It is worth mentioning that the adsorbent in this work is a kind of solid waste, the exploration of CGS is beneficial for resource utilization and environmental protection. The CGS has potential advantages in CW treatment due to the features of low cost and simple operation process.

4 Conclusion

CGS can be used as effective adsorbent to treat CW after pretreatment, the conclusions are as follows:

1. The pretreatment method of CGS was determined, CGS-F was selected to experience the HCl dipping process, and the volatile phenol removal rate from DCW of Ac-CGS-F125 was 48.90%. The sulfuric acid (3.0 M) dosage was 4.0 mL in acid precipitation process, and the volatile phenol removal rate was 15.81%.
2. The response surface designs were adopted to optimize the adsorption process, the highest volatile phenol removal rate of 69.7% was obtained by Ac-CGS-F150 with the optimal conditions as: pH of 3, $V_{L/S}$ of 3, processing time of 5.0 h, and particle size of 150 μm.
3. Batch experiment improved the volatile phenol removal rate to 85.1% in the third batch, the removal rate of NH_3–N and COD were 41.6% and 77.3%. Multi-grade batch process enhanced the pollutants removal rate. In grade 3 process, the volatile phenol removal rate reached 98.5%, and the removal rate of NH_3–N and COD were 73.6% and 80.5%. The color of water was clear and transparent.
4. Compared to similar adsorption studies of CW, the removal rate of volatile phenol and COD has great advantages of Ac-CGS-F125, the CGS has potential utilization in CW treatment due to its features of low cost and simple operation process.

Funding information: The financial support was obtained from the National Natural Science Foundation of China (22065035), Joint foundation of Clean Energy Innovation Institute and Yulin University (Grant. YLU-DNL Fund 2021003), and Science and Technology Foundation of Yulin (CXY202110104).

Author contributions: Ting Su: writing – original draft and writing – review and editing; Bozhou Xianyu: editing; Wenwen Gao: data curation and software; Yanli Gao: formal analysis and investigation; Pingqiang Gao: conceptualization and methodology; Cuiying Lu: project administration and visualization.

Conflict of interest: Authors state no conflict of interest.

Data availability statement: All data generated or analyzed during this study are included in this published article and its appendix.

References

[1] National Bureau of Statistics of China; 2022. http://www.stats.gov.cn.

[2] Hao X, Pan G, Ma C, Wei Y, Chen Z. Failure behavior and energy storage and release of hard coal under different static and dynamic loading states. Adv Civ Eng. 2020;2020:1–14.

[3] Guan WH, Gu CL, Lin ZS. Study on the change of energy consumption structure in China. J Nat Resour. 2006;21(3):401–7.

[4] Lan C, Lyu Q, Qie Y, Jiang M, Liu X, Zhang S. Thermodynamic and kinetic behaviors of coal gasification. Thermochim Acta. 2018;666:174–80.

[5] Ren J, Li J, Li J. Tracking multiple aromatic compounds in a full-scale coking wastewater reclamation plant: Interaction with biological and advanced treatments. Chemosphere. 2019;222:431–9.

[6] Elawwad A, Naguib A, Abdel-Halim H. Modeling of phenol and cyanide removal in a full-scale coke-oven wastewater treatment plant. Desalin Water Treat. 2020;57(52):25181–93.

[7] Bu Q, Li Q, Cao Y, Cao H. A new method for identifying persistent, bioaccumulative, and toxic organic pollutants in coking wastewater. Process Saf Env Prot. 2020;144:158–65.

[8] Yu X, Wei C, Wu H, Jiang Z, Xu R. Improvement of biodegradability for coking wastewater by selective adsorption of hydrophobic organic pollutants. Sep Purif Technol. 2015;151:23–30.

[9] Kong Q, Wu H, Liu L, Zhang F, Preis S, Zhu S. Solubilization of polycyclic aromatic hydrocarbons (PAHs) with phenol in coking wastewater treatment system: Interaction and engineering significance. Sci Total Environ. 2018;628–629:467–73.

[10] Wei C, Wei J, Kong Q, Fan D, Qiu G, Feng C. Selection of optimum biological treatment for coking wastewater using analytic hierarchy process. Sci Total Environ. 2020;742:140400.

[11] Chu L, Wang J, Dong J, Liu H, Sun X. Treatment of coking wastewater by an advanced Fenton oxidation process using iron powder and hydrogen peroxide. Chemosphere. 2012;86(4):409–14.

[12] Yin N, Yang G, Zhong Z, Xing W. Separation of ammonium salts from coking wastewater with nanofiltration combined with diafiltration. Desalination. 2011;268(1):233–7.

[13] Wang J, Ji Y, Zhang F, Wang D, He X, Wang C. Treatment of coking wastewater using oxic-anoxic-oxic process followed by coagulation and ozonation. Carbon Resour Convers. 2019;2:151–6.

[14] Raper E, Fisher R, Anderson DR, Stephenson T, Soares A. Nitrogen removal from coke making wastewater through a predenitrification activated sludge process. Sci Total Env. 2019;666:31–8.

[15] Ji Q, Tabassum S, Hena S, Silva CG, Yu G, Zhang Z. A review on the coal gasification wastewater treatment technologies: Past, present and future outlook. Clean Prod. 2016;126:38–55.

[16] Zhang M, Yang Q, Zhang J, Wang C, Wang S, Peng Y. Enhancement of denitrifying phosphorus removal and microbial community of long-term operation in an anaerobic anoxicoxic–biological contact oxidation system. Biosci Bioeng. 2016;122:456–66.

[17] Yang Q, Xiong P, Ding P, Chu L, Wang J. Treatment of petrochemical wastewater by microaerobic hydrolysis and anoxic/oxic processes and analysis of bacterial diversity. Bioresour Technol. 2015;196:169–75.

[18] Zhou H, Wei C, Zhang F, Liao J, Hu Y, Wu H. Energy-saving optimization of coking wastewater treated by aerobic biotreatment integrating two-stage activated carbon adsorption. J Clean Prod. 2018;175:467–76.

[19] Wang J, Ji Y, Zhang F, Wang D, He X, Wang C. Treatment of coking wastewater using oxic-anoxic-oxic process followed by coagulation and ozonation. Carbon Resour Convers. 2019;2:151–6.

[20] Hayes EK, Stoddart AK, Gagnon GA. Adsorption of SARS-CoV-2 onto granular activated carbon (GAC) in wastewater: Implications for improvements in passive sampling. Sci Total Environ. 2022;847:157548.

[21] Liu Z, Huang X, Miao Y, Gao B, Shi Y, Zhao J, et al. Eggplant biomass based porous carbon for fast and efficient dye adsorption from wastewater. Ind Crop Products. 2022;187:115510.

[22] Denga R-M, Avhafunani M, Mapula LM, Richard M. Activated carbon derived from waste orange and lemon peels for the adsorption of methyl orange and methylene blue dyes from wastewater. Heliyon. 2022;8(8):09930.

[23] Jiwon C, Neha S, Minyoung K, Kyusik Y. Activated carbon derived from sucrose and melamine as low-cost adsorbent with fast adsorption rate for removal of methylene blue in wastewaters. J Water Process Eng. 2022;47:102763.

[24] Shameran JS, Aram Salahuddin AK. Sewgil Saaduldeen Anwer, Adsorption of anionic dyes from textile wastewater utilizing raw corncob. Heliyon. 2022;8:10092.

[25] Chenglong X, Yali F, Haoran L, Yi Y, Ruifeng W. Research progress of phosphorus adsorption by attapulgite and its prospect as a filler of constructed wetlands to enhance phosphorus removal from mariculture wastewater. J Environ Chem Eng. 2022;10(6):108748.

[26] Kehan X, Long L, Zuohua H, Zhenbang T, Hui L. Efficient adsorption of heavy metals from wastewater on nanocomposite beads prepared by chitosan and paper sludge. Sci Total Environ. 2022;846:157399.

[27] Wenbo W, Aiqin W. Perspectives on green fabrication and sustainable utilization of adsorption materials for wastewater treatment. Chem Eng Res Des. 2022;187:541–8.

[28] Bingbing Q, Qianni S, Jicheng S, Chenhao Y, Huaqiang C. Application of biochar for the adsorption of organic pollutants from wastewater: Modification strategies, mechanisms and challenges. Sep Purif Technol. 2022;300:121925.

[29] Hongting W, Li Y, Yuanhang Q, Zhen C, Tielin W, Wei S, et al. Highly effective removal of methylene blue from wastewater by modified hydroxyl groups materials: Adsorption performance and mechanisms. Colloids Surf A Physicochem Eng Aspects. 2023;656:130290.

[30] Zhi L, Xiaohai H, Yi M, Bing G, Yiling S, Jianghui Z, et al. Eggplant biomass based porous carbon for fast and efficient dye adsorption from wastewater. Ind Crop Products. 2022;187:115510.

[31] Erto A. A comparison between a low-cost sorbent and an activated carbon for the adsorption of heavy metals from water. Water Air Soil Pollut. 2013;224:15314.
[32] Li P, Ailijiang N, Cao X, Lei T, Liang P, Zhang X. Pretreatment of coal gasification wastewater by adsorption using activated carbons and activated coke. Colloids Surf A Physicochem Eng Aspects. 2015;482:177–83.
[33] Zheng M, Han Y, Xu C, Zhang Z, Han H. Selective adsorption and bioavailability relevance of the cyclic organics in anaerobic pretreated coal pyrolysis wastewater by lignite activated coke. Sci Total Environ. 2019;653:64–73.
[34] Gao Q, Jin P, Wang L, Xing Y, Gui X, Van Puyvelde P. Removal of organic pollutants in coking wastewater based on coal-based adsorbents: A pilot-scale study of static adsorption and flotation. J Environ Chem Eng. 2021;9(6):106844.
[35] Azari A, Nabizadeh R, Mahvi AH, Nasseri S. Integrated Fuzzy AHP-TOPSIS for selecting the best color removal process using carbon-based adsorbent materials: multi-criteria decision making vs systematic review approaches and modeling of textile wastewater treatment in real conditions. Int J Environ Anal Chem. 2020;1–16. doi: 10.1080/03067319.2020.1828395.
[36] Peng B, Guo D, Qiao H. Bibliometric and visualized analysis of China's coal research 2000–2015. J Clean Prod. 2018;197:1177–89.
[37] Wang N, Sun X, Zhao Q, Yang Y, Wang P. Leachability and adverse effects of coal fly ash: A review. J Hazard Mater. 2020;396:122725.
[38] Wang N, Zhao Q, Xu H, Niu W, Ma L, Lan D. Adsorptive treatment of coking wastewater using raw coal fly ash: Adsorption kinetic, thermodynamics and regeneration by Fenton process. Chemosphere. 2018;210:624–32.
[39] Wu H, Lye LM, Chen B. A design of experiment aided sensitivity analysis and parameterization for hydrological modeling. Can J Civ Eng. 2012;39(4):460–72.
[40] Azari A, Mesdaghinia A, Ghanizadeh G, Masoumbeigi H, Pirsaheb M, Ghafari HR. Which is better for optimizing the biosorption process of lead - central composite design or the Taguchi technique? Water Sci Technol. 2016;74(6):1446–56.
[41] Porto IS, Neto JHS, dos Santos LO, Gomes AA, Ferreira SL. Determination of ascorbic acid in natural fruit juices using digital image colorimetry. Microchem J. 2019;149:104031.
[42] Acikkapi AN, Tuzen M, Hazer B. A newly synthesized graft copolymer for magnetic solid phase microextraction of total selenium and its electrothermal atomic absorption spectrometric determination in food and water samples. Food Chem. 2019;284:1–7.
[43] Kiani A, Ahmadloo M, Moazzen M, Shariatifar N, Shahsavari S, Arabameri M. Monitoring of polycyclic aromatic hydrocarbons and probabilistic health risk assessment in yogurt and butter in Iran. Food Sci Nutr. 2021;9(4):2114–28.
[44] El-Sayed EM, Hamad HA, Ali RM. Journey from ceramic waste to highly efficient toxic dye adsorption from aqueous solutions via one-pot synthesis of $CaSO_4$ rod-shape with silica. J Mater Res Technol. 2020;9(6):16051–63.
[45] Na LI, Almarri M, Ma Xl, Zha QF. The role of surface oxygen-containing functional groups in liquid-phase adsorptive denitrogenation by activated carbon. New Carbon Mater. 2011;26(6):470–8.
[46] Xu C, Sun WZ, Qin XL, Jia YX, Yu ST, Xian M. Effective adsorption of phenolic compounds by functional group modified resins: behavior and mechanism. Sep Sci Technol. 2019;54(4):467–77.
[47] Jain SN, Tamboli SR, Sutar DS. Batch and continuous studies for adsorption of anionic dye onto waste tea residue: kinetic, equilibrium, breakthrough and reusability studies. J Clean Prod. 2020;252:119778.
[48] An W, Yang T, Wang Y, Xu J, Hu J, Cui W. Adsorption and *in situ* photocatalytic Fenton multifield coupled degradation of organic pollutants and coking wastewater via FeBiOBr modification of three-dimensional graphene aerogel. Appl Surf Sci. 2023;610:155495.
[49] Zhang X, Li Y, He Y, Kong D, Klein B, Yin S. Co-pyrolysis characteristics of lignite and biomass and efficient adsorption of magnetic activated carbon prepared by co-pyrolysis char activation and modification for coking wastewater. Fuel. 2022;324:124816.
[50] Zhang Y, Qin L, Cui Y, Liu WF, Liu XG, Yang YZ. A hydrophilic surface molecularly imprinted polymer on a spherical porous carbon support for selective phenol removal from coking wastewater. New Carbon Mater. 2020;35(3):220–31.

Appendix

Table A1: Factors and levels for the experimental design

Factor	Levels		
	1	2	3
A (–)	3	5	8
B (–)	1	2	3
C (h)	3	5	7
D (μm)	180	150	125

Table A2: Orthogonal array for the experiment

No.	A	B	C	D
1	1	1	1	3
2	3	1	1	3
3	3	3	2	1
4	2	2	3	3
5	1	3	1	1
6	2	3	2	1
7	1	1	2	1
8	1	3	2	2
9	3	3	2	2
10	2	1	1	1
11	1	2	2	1
12	2	1	2	2
13	2	3	2	3
14	2	2	1	2
15	3	1	2	1

Table A3: Analysis of variance for the regression model (R^2 = 0.9955)

Source	D_f	Sum of square	Mean square	F value	P value
Model	12	125.346	10.446	37.0758	0.0266
Error	2	0.564	0.282		
Total	14	125.909			

Table A4: Significance test for the regression coefficients

Source	D_f	Sum of square	F value	P value
A	1	58.0787	206.1477	0.0048*
B	1	15.8915	56.4062	0.0173*
C	1	0.4950	1.7570	0.3161
D	1	0.1489	0.5285	0.5428
A × A	1	1.9811	7.0319	0.1176
A × B	1	6.9147	24.5436	0.0384*
B × B	1	3.5156	12.4784	0.0716
A × C	1	0.0740	0.2628	0.6592
B × C	1	0.4537	1.6103	0.3321
B × D	1	0.0386	0.1370	0.7468
C × D	1	0.5324	1.8897	0.3030
D × D	1	7.1218	25.2786	0.0374*

"*" means significant influence factor.